Hydrogen Bonds in NH_4F and NH_4HF_2 Crystals. Comparison of Electron Density Distribution Obtained by X-ray Diffraction and by Quantum Chemistry

Sikko J. van Reeuwijk, Kai G. van Beek, and Dirk Feil*

Chemical Physics Laboratory, University of Twente, POB 217, 7500 AE Enschede, The Netherlands

Received: May 11, 2000; In Final Form: August 28, 2000

The quality of the Hartree−Fock and the density functional methods for the description of hydrogen bonds is judged by comparing quantitatively the outcome of calculations on the hydrogen bonds in ammonium (bi)fluorides with the results of accurate electron density studies by X-ray diffraction. X-ray data and analysis for NH_4F were taken from the literature; those for NH_4HF_2 were collected in a single-crystal diffraction experiment. A total of 8522 reflections was measured, yielding the structure factors of 2333 independent reflections. R_{int} (F^2) = 0.03. A multipole refinement converged to R_w (F^2) = 0.034. Quantum chemical calculations were carried out with the CRYSTAL package, using the Hartree−Fock and the density functional methods and a 6-311G** basis set. Both the local density and the generalized gradient(GGA) version of the latter were applied. To make a comparison with experiment valid, the theoretical densities were converted to structure factors that then were subjected to the same multipole refinement as the experimental ones. The differences between the theoretical and the experimental results are shown by comparing in direct space the electron density in the bonding regions in the crystals and the topological characteristics at the bond critical points, in reciprocal space the structure factors as functions of the scattering angle. The GGA results showed the best agreement with experiment, with excellent agreement both in the very short and the longer hydrogen bonds. The curvatures of the electron density distributions along the hydrogen bonds and perpendicular to it reveal the character of these bonds.

Introduction

The electron density distribution (EDD) in a system determines many chemical and physical phenomena, for example, intermolecular forces, molecular geometry, electrostatic potential, and chemical bonding. The EDD can be calculated from first principles, or ab initio, using quantum mechanical methods. In the past few decades, many computer programs have been developed to do so, most of which calculate the EDD from the wave function, which, in turn, results from solving the Schrödinger equation. Because for only very few systems the Schrödinger equation can be solved analytically, adequate approximations are required. A well-known example of this is the Hartree−Fock (HF) theory (restricted or unrestricted) to approximate molecular wave functions. An alternative method, the density functional theory (DFT), is based on the EDD rather than on the wave function. It has been integrated into several ab initio programs. One of these programs is CRYSTAL95,[1] which includes the periodicity of a crystal in the calculation. From these calculations one can extract physical properties of the crystal, like band spectra (associated to the band gaps) and bond energies. Comparison of theoretical values with experimental ones shows the strengths and the weaknesses of the various methods; hence comparisons between these values are often made. Less frequently, we find comparisons of the basic quantity, the EDD itself, with experimental values as obtained from X-ray diffraction. In the present paper we aim to do so. We focus our attention in particular on the effect of hydrogen bond formation, which is most notable in the diffuse regions between atoms. Gatti et al. showed that placing a molecule in a periodic lattice causes changes in the EDD in diffuse regions.[2] In a previous study[3] we showed the suitability of the DFT by means of a comparison of ab initio calculations and X-ray diffraction results for urea, the compound that was studied by Gatti et al. It is not clear yet whether the HF and the DFT methods, both of which are coded in CRYSTAL95, yield good results in diffuse regions subject to rather strong internal electric fields.

A fruitful method for characterizing bonds is Bader's method, which focuses on the electron density distribution about the critical points along the bond path.[4] In addition to these comparisons in direct space, we will also make a confrontation in reciprocal space by comparing the structure factors.

We have chosen ammonium fluoride, NH_4F, and ammonium hydrogen bifluoride, NH_4HF_2, as subjects of our study for several reasons: (1) in these systems with molecular ions we can expect to find strong electrostatic fields perturbing the electronic structure of the molecular constituents; (2) with seven or less atoms in the asymmetric unit, the system is sufficiently small to be handled quantum chemically with a sufficiently large basis set; (3) accurate experimental neutron data are available for both structures and one of us had determined the X-ray structure of NH_4F.[5] Even more important is the fact that the structures contain a number of widely different hydrogen bonds, ranging from the moderately strong, mainly electrostatic hydrogen bond in NH_4F to the strong bond in the hydrogen bifluoride ion, [F−H−F], with its ambiguous character, in NH_4HF_2. In fact the hydrogen bond in the latter group is generally accepted as the strongest known hydrogen bond.[6] A direct measurement of the bonding energy of the hydrogen bond in hydrogen bifluoride ion by ion cyclotron experiments yielded

* Author for correspondence. Fax: +31-53-489 4738; e-mail: d.feil@ct.utwente.nl.

10.1021/jp001747e CCC: $19.00
Published on Web 11/01/2000

SCHEME 1[a]

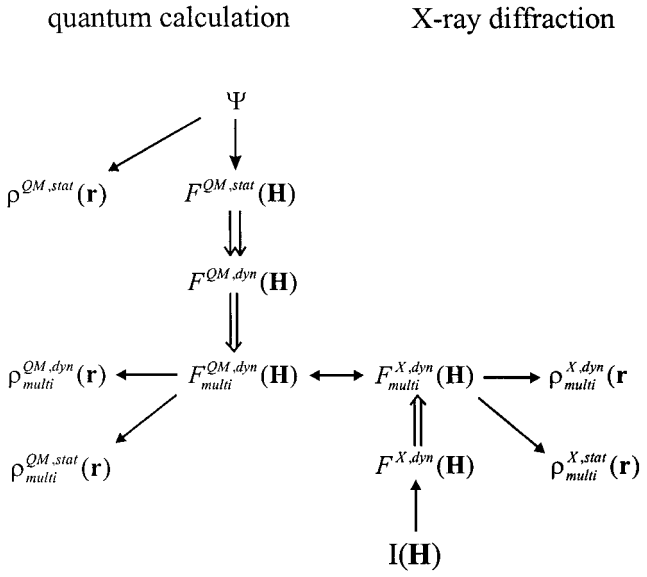

[a] Ψ, $\rho^{QM,stat}(\mathbf{r})$, $F^{QM,stat}(\mathbf{H})$ are the wave function, the electron density distribution (EDD), and the structure factors as calculated with the quantum chemical program; $F^{QM,dyn}(\mathbf{H})$ are the structure factors of the thermally smeared EDD; $F^{QM,dyn}_{multi}(\mathbf{H})$, $F^{X,dyn}_{multi}(\mathbf{H})$ are the modeled dynamic structure factors from theory and experiment respectively; $\rho^{QM,stat}_{multi}(\mathbf{r})$, $\rho^{X,stat}_{multi}(\mathbf{r})$, $\rho^{QM,dyn}_{multi}(\mathbf{r})$, $\rho^{X,dyn}_{multi}(\mathbf{r})$ are the static and the dynamic EDDs as calculated from the multipole functions; $I(\mathbf{H})$ are the observed intensities in the diffraction experiment; ⇊ is the thermal smearing operation, discussed below, resulting in the dynamic structure factors $F^{QM,dyn}$; ↓,↑, indicate modeling with the help of a multipole refinement (with the POP program); ↔, comparison of theory and experiment.

a bonding energy of 163(4) kJ/mol.[7] The fact that several interesting features occur in groups that are chemically very similar, but crystallographically independent, increases the value of the comparison. Furthermore it is reported that most variants of DFT yield a proton-transfer barrier in $(F\cdots H\cdots F)^-$ that is considerably smaller than the best-correlated conventional ab initio results, with a large polarized basis set.[8] This suggests differences in the outcome of the electron density calculations.

Before the results are given, the methods used are shortly discussed in the following section.

Methods

Comparisons. The various quantities that will be compared and their relation to the quantum chemical calculations and to the experimental data are given in Scheme 1. The quantum chemical results are based on a static structure, whereas the experimental data refer to a structure with thermal motion. This requires a procedure to apply the effects of thermal motion to the static EDDs. Furthermore, the experimental data were fitted to a multipole model using a least-squares refinement program (see multipole refinement below). These programs reduce the influence of noise and ripple effects caused by a limited set of diffraction intensities. However, they act as a filter and introduce systematic errors, the refinement bias. To make the comparison valid, the same bias should be introduced in the theoretical data. The various quantities and their relations are given in Scheme 1.

Multipole Modeling. The EDD, obtained from the X-ray experiment or from a quantum chemical calculation, is often modeled with the help of multipole distributions.[9] For the present purpose a short description suffices.

The crystalline EDD is written as a linear combination of atomic EDDs, which in turn are written as sum of a core and a valence density.

$$\rho(\mathbf{r}) = \sum_a \rho_a(\mathbf{r}) = \sum_a [\rho_a^{core}(r) + \rho_a^{valence}(\mathbf{r})] \quad (1)$$

The first one is assumed to remain unchanged during bonding, whereas the second depends on the environment of the atom concerned.

$$\rho_a^{valence}(r) = p_a^{val}\sum_k R_k(r;\kappa\alpha_k) + \sum_{l=1}^{4}\sum_{m=-1}^{l} C_{p,l,m} R_n(r;\alpha_a) Y_{l,m}(\theta,\phi) \quad (2)$$

where the radial function used is given by

$$R_n(r;\alpha) = \frac{\alpha^{n+3}}{4\pi(n+2)!} r^n e^{-\alpha r} \quad (3)$$

and κ is a contraction parameter.

Stewart and co-workers have tabulated α values for many atoms.[10]

To model an experimental EDD, a limited number of deformation functions is used to prevent the incorporation of noise in the result. Hence the model density differs slightly from the original one and a bias is introduced. In most cases of modeling on basis of accurate diffraction data, multipole functions are used up to hexadecapole functions for the fluoride and nitrogen atoms, and up to quadrupole functions for the hydrogen atoms. In these expressions, the atomic EDDs represent static densities, that is, EDDs of atoms at rest. The atoms that make up the crystal, however, are subject to thermal motion, and a temperature factor has to be introduced. The multipole method assumes rigid atoms; hence we can write the dynamic or thermally smeared EDD as a convolution:

$$\rho_a^{dyn} = \rho_a^{stat} \otimes pdf_a \quad (4)$$

in which pdf_a is the probability density function of nucleus a. When harmonic motion is assumed, it requires six thermal parameters to describe this three-dimensional Gaussian function. Symmetry often reduces this number. Contraction, or rather its inverse, expansion, and thermal motion have similar effects on the scattering factor, that is, reduction at high scattering angles. It can be expected that in refinements of experimental data uncoupling of the two is hard to obtain.

When the model is fitted to an EDD, the sum-weighted differences between squared structure factors is minimized, rather than the difference between the model and the reference EDD. Hence important input in the refinement procedure is the set of structure factors and the weight that is assigned to each of them. Thus in the refinement of the theoretical data set we use only those structure factors that were measured in the experiment and apply the experimental weight factor of each reflection to make sure that the systematic errors are closely similar to the ones introduced in the refinement of the experimental data.

Thermal Smearing. A calculation (HF or DFT) with the CRYSTAL95 program provides us with a set of structure factors corresponding to a static EDD. Lattice vibrations of the crystal that consist of zero point vibrations and thermal excitations cannot be taken into account. In principle, it is possible to calculate the EDD at a finite temperature by calculating the wave function for all excited states and making a Boltzmann distribution over all these states, but in practice the procedure is unfeasible. We have approximated the influence of the lattice

vibrations by applying the Debye−Waller factor, obtained from the X-ray diffraction experiment, to the quantum chemical EDD. In a first step the crystalline EDD is partitioned into atomic EDDs by the stockholder method.[11] These atomic fragments are assumed to be rigid: the electron density cloud follows the nucleus during its thermal motion without being deformed. In a second step the atomic EDD is written as the sum of a core density and a linear combination of multipole densities, as described in the previous section. Because the EDD is precisely known, the fit can be made with any desired accuracy and this time the number of parameters greatly exceeds the number that is used in modeling experimental data. The convolution of the modeled EDD with the probability density function of the nucleus is carried out by Fourier transformation. A detailed account of the method is given by Bruning and Feil.[12] It turns out, however, that it is not necessary to use a very extensive model to represent the theoretical EDD; the models used to describe the experimental EDDs suffice. Hence the following procedure is used as well: the structure factors resulting from the quantum chemical calculation are used in a refinement procedure in which each reflection has the same weight. In the refinement the positions of the atoms are kept fixed and only the multipole parameters are varied. After convergence we have at our disposal the set of structure factors $F_{\text{fit}}^{\text{QM,stat}}(\mathbf{H})$. Subsequently the thermal parameters are set to the values obtained in the refinement of the experimental data and the structure factors are calculated again, yielding the set $F_{\text{fit}}^{\text{QM,dyn}}(\mathbf{H})$. The theoretical dynamic structure factors are then calculated according to

$$|F^{\text{QM,dyn}}(\mathbf{H})| = |F^{\text{QM,static}}(\mathbf{H})| * \frac{|F_{\text{fit}}^{\text{QM,dyn}}(\mathbf{H})|}{|F_{\text{fit}}^{\text{QM,stat}}(\mathbf{H})|} \qquad (5)$$

The two methods yielded results that were practically the same. As was stated above, uncoupling of thermal and contraction parameters is difficult. Therefore the valence shell contraction parameters, κ, are fixed to the values as determined from the refinement of the experimental data. This, in fact, is another condition to be satisfied when using the Debye−Waller factor as we did in eq 5.

To introduce the refinement bias in the theoretical data, we assign the experimental weights to $F^{\text{QM,dyn}}(\mathbf{H})$ and subject them to a new least-squares refinement, resulting in $F_{\text{model}}^{\text{QM,dyn}}(\mathbf{H})$. The EDDs, corresponding to the multipole models fitted to the experimental structure factors on one hand, and to the dynamic, theoretical structure factors at the other, $\rho_{\text{multi}}^{\text{X,stat}}(\mathbf{r})$ and $\rho_{\text{multi}}^{\text{QM,stat}}(\mathbf{r})$ respectively, can now be compared. The same applies to the structure factors calculated from the modeled densities. Because in both theory and experiment the same modeling is applied, the same systematic errors are expected to occur.

X-ray Diffraction Studies

NH_4F. In 1927, Zachariasen determined the arrangements of the N/F framework in NH_4F.[13] The structure is hexagonal in the polar space group $P6_3mc$, the well-known wurzite structure. The positions of the hydrogen atoms were determined by Adrian and Feil, using both X-ray and neutron diffraction.[14] The unit cell contains two ammonium fluoride groups (Figure 1). As a consequence of the space group, the N, F, and one of the H atoms lie on the polar axis, whereas the other three hydrogen atoms occupy equivalent positions. Thus the asymmetric unit is made up of the four atoms, F, N, H1, and H2. The structure was studied again by van Beek et al. to obtain an accurate

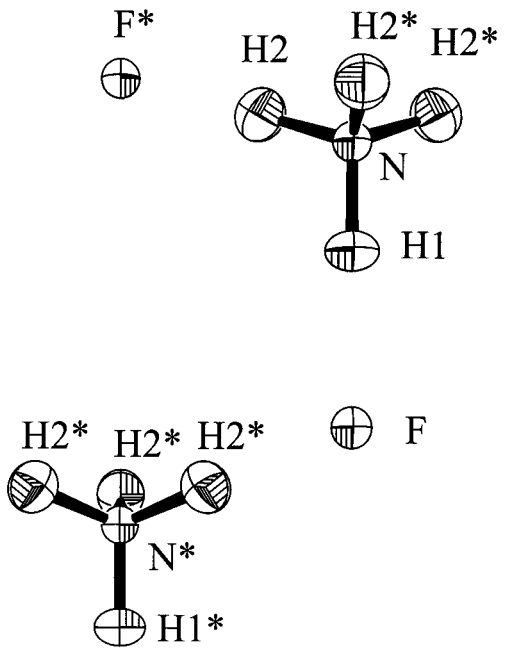

Figure 1. ORTEP drawing of ammonium fluoride showing 50% probability mean-square displacement ellipsoids of the atoms at 120 K. Atoms labeled with an asterisk are generated by crystallographic symmetry. The crystallographic *c*-axis runs from the bottom to the top of the figure.

description of the EDD.[5] In this study the fluorine ion was kept spherical. The reason for this approach was the fact that certain antisymmetric deformation functions strongly correlate with the choice of origin in the polar space group, yielding large deformation parameters, whereas the deformation itself can be assumed to be small for chemical reasons. Similar effects were found and discussed by Craven and co-workers[15] and Hansen and co-workers.[16] When quantum chemical calculations, however, showed some tetrahedral deformation, the refinement of the experimental data was repeated, this time with tetrahedral deformation functions, constructed from the octopolar functions o_2 and o_7, added to the refinement model. The refinement converged to $R_w(F^2) = 0.040$ and $R(F^2) = 0.017$ and goodness-of-fit = 1.00. After the refinement there were 37.7(3) electrons in the unit cell as compared with 40 for a neutral cell. The final values of the pseudo-atom parameters corresponding to a neutral cell are given in Table 1.

NH_4HF_2. The structure of ammonium hydrogen bifluoride was first solved by Pauling, who proposed the centrosymmetric space group *Pman*.[17] An X-ray diffraction study by McDonald confirmed the proposed space group.[18] When this author noted a slightly different thermal motion in one of the two chemically similar FHF groups, he attributed this to experimental errors. However, the position of the hydrogen atoms in the crystallographically different hydrogen bifluoride groups (and thus the space group) remained subject to much debate. Recently, a neutron diffraction study by Van Beek et al.[19] supported space group *Pman*. To comply with previous work, this nonstandard setting of space group *Pmna* (#53) has been used throughout the current study. The equivalent positions of this space group are

$$\pm\left(x, y, z; x, -y, -z; \frac{1}{2} - x, \frac{1}{2} - y, z; \frac{1}{2} - x, \frac{1}{2} + y, -z\right)$$

A quarter of the unit cell of ammonium hydrogen bifluoride in this space group is shown in Figure 2. The $b-c$ plane is a

TABLE 1: Pseudo-Atom Parameters in NH_4F, using Tetrahedrally Deformed F Atoms

	atom			
parameter	F	N	H1	H2
x	1/3	1/3	1/3	0.4614(8)
y	2/3	2/3	2/3	0.5386
z	0	0.3777(1)	0.2337(10)	0.4270(5)
U_{11}	0.0155(3)	0.0144(4)	0.028(3)	0.0256(8)
U_{22}	0.0155	0.0144	0.028	0.0256
U_{33}	0.0163(4)	0.0149(5)	0.015(4)	0.027(4)
U_{12}	0.0077	0.0072	0.014	0.0164(8)
U_{13}				−0.0012(9)
U_{23}				0.0012
p_v	7.64(10)	5.3(2)	0.81(6)	0.74(3)
d_1				−1.6(3)
d_2				0.9
d_3		0.2(5)	2.2(5)	−0.7(2)
q_5		0.0(4)		
o_2	−0.8(2)	−1.4(3)		
o_7	0.5	−1.9(4)		
κ	1.036(6)	1.018(14)		

[a] Labeling of atoms in the asymmetric unit conforms to previous work, referred to in the text. Positional parameters x,y,z are fractional coordinates in the unit cell. Mean-square displacement parameters U_{ij} are given in Å^2 units and correspond to the expression $T = \exp(-2\pi^2\sum_{ij}h_ih_ja^{*i}a^{*j}U_{ij})$. Values vanishing by symmetry or by the model used are left empty. Values without estimated standard deviation are derived from symmetry-related values. Positional and mean-square displacement parameters of the hydrogen atoms are taken from the previous neutron diffraction study of Adrian and Feil.[14] Electron population parameters p_v, d_1, etc. correspond to normalized multipole population parameters and are referred to crystal cartesian axes a, b^*, c.

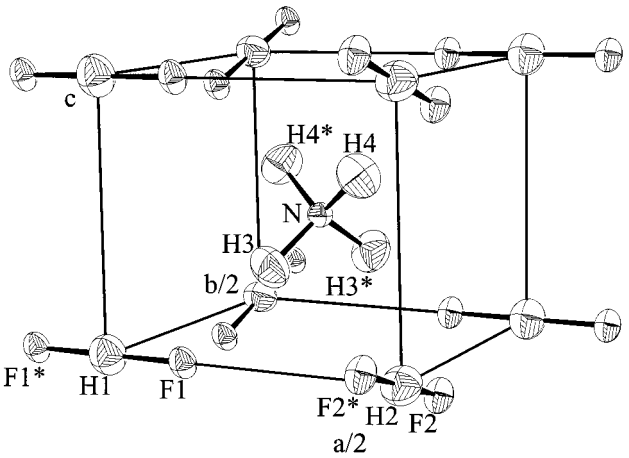

Figure 2. A quarter of the unit cell of NH_4HF_2 showing 50% probability thermal motion. The origin is in the H1 atom. Atoms not labeled or indicated by an asterisk are generated by symmetry operations.

mirror plane. The a-axis and the axis through the N atom, parallel to the c-axis, are twofold rotation axes. These symmetry elements determine the site symmetry of the various atoms of the structure. The asymmetric unit of ammonium hydrogen bifluoride contains two crystallographically different hydrogen bifluoride groups. By symmetry, the two F atoms in the FHF groups are equivalent. Furthermore, the ammonium group contains two crystallographically different hydrogen atoms. To obtain an accurate electron density distribution, we measured X-ray diffraction intensities and applied a multipole analysis.

Measurements. Crystals were grown in the same manner as the crystals used for neutron diffraction. A crystal of dimensions $0.30 \times 0.27 \times 0.20$ mm^3 was selected and mounted on a glass fiber with the c-axis close to the ϕ axis of the Nonius CAD4 diffractometer. To minimize ice formation on the crystal during cooling, the diffractometer was placed in a sealed box with a constant supply of dry air into the box. The crystal was kept at a nominal temperature of 102 K in a stream of nitrogen gas. Throughout the data collection, the temperature was monitored (±1 K) using a thermocouple located about 8 mm upstream from the crystal. X-ray diffraction data were collected using niobium-filtered MoKα radiation, $\lambda = 0.71069$ Å. Unit cell dimensions, Table 2, were obtained from a least-squares fit of $\sin^2\theta_{hkl}$ for 25 reflections spread throughout reciprocal space measured at four symmetry equivalent positions.

TABLE 2: Unit Cell Dimensions (Å) for NH_4HF_2 at 100 K as Determined from Neutron and X-ray Diffraction

	a	b	c
neutron	8.412(10)	8.184(10)	3.615(15)
X-ray	8.380(3)	8.162(2)	3.6200(7)

Bragg reflection intensities were measured using $\omega/2\theta$ scans for all reflections with $H \equiv \sin\theta/\lambda \leq 1.29$ Å^{-1} in a hemisphere of reciprocal space ($|h| \leq 21$, $|k| \leq 21$, $l \leq 9$). The intensities of three monitor reflections were measured every 6000 s of the data collection. Integrated intensities were obtained from the collected scan profiles using the method of Lehmann and Larsen[20] and the data processing programs of Blessing.[21] The integrated intensities were internally scaled by factors ranging from 0.969 to 1.050 that were obtained from the observed variations of the monitor reflections during the course of the data collection. An absorption correction ($\mu = 0.1923$ mm^{-1}) was applied, giving correction factors from 0.946 to 0.964. A total of 8522 reflections was collected; averaged symmetry equivalent reflections gave 2333 independent reflections with an internal agreement factor of $R_{int}(F^2) = 0.029$. The details of experiment and refinement, and the definitions of the various agreement factors, are collected in Table 3.

Results from Neutron Study. We also performed a neutron study to support the X-ray analysis. The details of this study will be published elsewhere, but here we summarize the salient facts needed for the present analysis.

The sample for data collection measured approximately 1.2 × 1.0 × 1.0 mm. Data were collected at 100(1) K on the SXD diffractometer at the ISIS pulsed-neutron source, using the time-of-flight Laue diffraction technique. The final unit cell dimensions are reported in Table 2, together with the X-ray results. The slight differences suggest that the temperatures were not quite as close as is claimed. A total of 5168 reflections was collected; averaging symmetry equivalent reflections gave 772 independent reflections with an internal agreement factor of $R_{int}(F^2) = 0.049$. Fourier maps of the observed reflections were calculated in the planes of both crystallographically independent hydrogen bifluoride ions. No evidence could be found for a double potential well in either F1−H1−F1 or F2−H2−F2. Subsequently, space group *Pman* was used throughout this study, and the hydrogen atoms H1 and H2 were fixed at their positions of 2/m symmetry.

Closer analysis of the Fourier density maps revealed anharmonic nuclear motion for atom F2. To model this motion, third-order displacement parameters as defined in the Gram−Charlier formalism were introduced for all fluoride and nitrogen atoms. The anharmonic third-order parameters of atoms F1 and N were within 1.5σ of zero and were subsequently set to zero. The refinement yielded no significant improvement according to Hamilton's criteria, but the residual density showed no structural features any more. Hence the results of the expanded model are used in the remainder of this study.

TABLE 3: Summary of Details of Data Collection and Refinement of NH_4HF_2

wavelength (Å)	0.71069
temperature (K)	102(1)
μ (mm^{-1})	0.1923
crystal size (mm^3)	$0.30 \times 0.27 \times 0.20$
scan type	$\omega - 2\theta$
$(\sin\theta/\lambda)_{max}$ ($Å^{-1}$)	1.29
indices range	
h	$-21 \rightarrow 21$
k	$-21 \rightarrow 21$
l	$0 \rightarrow 9$
number of reflections	
measured	8522
unique	2333
$R_{int}(F^2)$	0.029
S, goodness-of-fit	1.05
$R(F^2)$	0.029
$R_w(F^2)$	0.034

$$R_{int}(F^2) = \frac{\sum_{H,i} |\langle F^2(H)\rangle - F_i^2(H)|}{\sum_{H,i} F_i^2(H)}$$

$$S = \sqrt{\frac{\sum_H w_H(|F_c(H)|^2/k - |F_o(H)|^2)^2}{m-p}}$$

$$R_w(F^2) = \sqrt{\frac{\sum_H w_H(|F_c(H)|^2/k - |F_o(H)|^2)^2}{\sum_H w_H(|F_o(H)|^2)^2}}$$

$$R(F^2) = \frac{\sum_H ||F_c(H)|^2/k - |F_o(H)|^2|}{\sum_H (|F_o(H)|^2)}$$

$$w_H = 1/\sigma^2(|F_o(H)|^2)$$

[a] m and p are the number of reflections and parameters, respectively.

Refinement of Structure from X-ray Diffraction Data. Because at high-order diffraction the scattering is hardly affected by multipole deformation of the atoms, a high-order refinement can be used to determine the thermal motion of the nonhydrogen atoms. This least-squares refinement of the X-ray diffraction data consisted of fitting a model to all 1766 reflections of the X-ray diffraction data that had $H > 0.8$ $Å^{-1}$. When it was realized that many of the reflections at high resolution were insignificant in terms of their standard deviation, the data set was truncated to reflections having $H \leq 1.00$ $Å^{-1}$ and intensity more than $3\sigma(F_o^2)$, leaving a data set of 822 reflections to be used to complete the high-order refinement. The model contained the overall scale factor and positional and mean-square displacement parameters for the F and N atoms and third-order displacement parameters as defined in the Gram−Charlier formalism for atom F2. Including third-order displacements for the other nonhydrogen atoms did not lead to any improvement, in agreement with the neutron results. The displacement parameters for the N and F atoms showed a significant difference with the results from the neutron refinement, these differences exceeding the values that can be expected from the minute difference in temperature. We submit that these differences find their origin in the different observation methods, with different accounts of background scattering and of thermal diffuse scattering. The limitation of scan angles leads to spectral truncation, which in turn causes systematic intensity errors. In structure refinements these errors find their way by adding a truncational component to the displacement factor.[22]

Hence a scale factor has to be applied before neutron displacement parameters can be applied in the X-ray refinement of the structure, in particular for the hydrogen atom, where high-order scattering is absent. The required scale factor was calculated as the ratio of the principal values of the mean-square displacement parameters of the nitrogen and fluoride atoms as determined from the analysis of the neutron diffraction data, and those obtained from the high-order least-squares refinement of the X-ray diffraction data. The calculated average scale factor, 1.38(4), was applied to the mean-square neutron displacement parameters of the hydrogen atoms and the resulting values were used in further refinement of the structure.

The electron density distribution in the crystal structure of ammonium hydrogen bifluoride was determined by multipole modeling using the program POP.[23] X-ray scattering factors for the pseudo-atom K-shells of N and F atoms were assumed to be those of isolated HF atoms. Scattering factors for the spherical component of the L-shell of the N and F atoms were constructed from a linear combination of Slater-type Roothaan−HF atomic wave functions. Higher multipole functions, as well as the radial scattering factor for the hydrogen atoms, were assigned a single Slater-type radial function. These functions had a fixed standard value for the radial component, $\alpha = 8.50$ $Å^{-1}$ for F and $\alpha = 7.37$ $Å^{-1}$ for N, values determined by Stewart and co-workers.[10] Initially a radial exponent of $\alpha = 4.69$ $Å^{-1}$ was assigned to all hydrogen atoms.

The positional and thermal parameters for the hydrogen atoms were taken from the neutron study. The function $\sum w\Delta^2$ was minimized, where $\Delta = |F_o^2| - |F_o^2|$ and $w = 1/\sigma^2(F_o^2)$.

The least-squares model fitted to all X-ray diffraction reflections consisted of the model as used for the high-order refinement, extended with contraction parameters κ(F), κ(N), monopole population parameters p^{val}, and all symmetry allowed higher multipole population parameters up to hexadecapole population parameters for F and N and up to quadrupole population parameters for H. An isotropic extinction parameter, g, assuming a type I crystal with Gaussian mosaicity was introduced.[24] Positional and scaled mean-square displacement parameters for the hydrogen atoms were kept fixed to their values as determined from the least-squares refinement of the neutron diffraction data. The third-order Gram−Charlier displacement parameters of atom F2 were fixed to the values as determined by the high-order least-squares refinement of the X-ray diffraction data. Again, reflections having $H > 1.00$ $Å^{-1}$ and intensity less than $3\sigma(F_o^2)$ were omitted from the refinement. We justify this choice by the consideration that the deformation density of the atoms involved scatters almost exclusively in this region in reciprocal space since no lone pairs are present. High-resolution data derive their undisputed usefulness from the increased quality of the deconvolution of thermal displacement and bonding deformation. In the present case the displacement parameters were derived from the neutron study with only the scale factor as parameter. The refinement was completed with the remaining 1383 reflections. Upon convergence, residual Fourier maps were calculated in the plane of each of the hydrogen bifluoride ions. A residual electron density of approximately 0.05 $eÅ^{-3}$ was noticed at the positions of the hydrogen atoms of the hydrogen bifluoride ions.

The used radial exponent of $\alpha = 4.69$ $Å^{-1}$ for the hydrogen

TABLE 4: Positional and Thermal Parameters from Multipole Analysis of NH_4HF_2

atom	F1	F2	N	H1	H2	H3	H4
x	0.1362(1)	0	0.25	0	0	0.2070(3)	0.1598(3)
y	0	0.3679(1)	0.25	0	0.5	0.1570(2)	0.2949(2)
z	0	0.8959(2)	0.4557(2)	0	0	0.2913(5)	0.6200(5)
U_{11}	133(1)	141(1)	125(2)	250(20)	260(20)	350(10)	280(10)
U_{22}	136(1)	143(1)	121(2)	260(20)	280(20)	249(9)	400(10)
U_{33}	199(1)	195(1)	111(2)	320(20)	230(10)	332(9)	323(9)
U_{12}	0	0	−8(2)	0	0	−57(8)	70(10)
U_{13}	0	0	0	0	0	−36(8)	79(8)
U_{23}	−45(1)	−55(1)	0	−40(10)	−40(10)	−62(7)	−43(7)
C_{222}		3(2)					
C_{333}		−110(4)					
C_{113}		0(3)					
C_{223}		−11(3)					
C_{233}		27(6)					

[a] The expression for thermal displacement is given by $T = \exp(-2\pi^2\sum_{ij}h_ih_ja^{*i}a^{*j}U_{ij})[1 - {}^4/_3\pi^3i\sum_{jkl}h_jh_kh_la^{*j}a^{*k}a^{*l}C_{jkl}]$. The mean square displacement parameters U_{ij} are given in $Å^2*10^{-4}$ units; the Gram−Charlier expansion coefficients C_{jkl} are given in $Å^3*10^4$. Parameter values without estimated standard deviations (in parentheses) are symmetry constrained.

TABLE 5: Bond Distances (Å) and Angles in NH_4HF_2 (degrees)

bond	distance	bond	distance
F1−H1	1.1412(8)	F1..(H1)..F1	2.282(2)
F2−H2	1.1421(8)	F2..(H2)..F2	2.284(2)
N−H3	1.030(2)	N..(H3)..F1	2.7919(6)
N−H4	1.030(2)	N..(H3)..F2	2.8027(9)
bond	**angle**	**bond**	**angle**
H3−N−H3	109.4(2)	N−H3···F1	178.5(2)
H3−N−H4	109.2(2)	N−H4···F2	178.2(2)
H4−N−H4	109.4(2)		

[a] In the hydrogen bonds of the second column the distances concern the two outer atoms.

atoms corresponds to the contracted EDD of a covalently bonded hydrogen atom. However, the hydrogen atoms of the hydrogen bifluoride ions are involved in a three-center bond with unknown effects on the EDD. Therefore these hydrogen atoms were assigned the radial exponent of an isolated hydrogen atom, $\alpha = 3.78$ Å^{-1}. Least-squares refinement was repeated with the above radial exponent for atoms H1 and H2. Upon convergence of the least-squares refinement, the residual electron density at the hydrogen positions of the hydrogen bifluoride ions was found to be insignificant. In subsequent least-squares refinements, a radial exponent of $\alpha = 3.78$ Å^{-1} was used for the hydrogen atoms of the hydrogen bifluoride groups. Convergence was obtained with $R_w(F^2) = 0.034$, $R(F^2) = 0.029$, and goodness-of-fit = 1.05. The final value of $g = 0.94(2)*10^{-4}$ rad^{-1} indicated that extinction effects were severe. The largest correction for a Bragg intensity was a decrease of 48%. Rejecting the seven reflections that had a decrease due to extinction effects in excess of 10% did not lead to significantly different least-squares parameters and was not pursued further. The final values for the pseudo-atom parameters are given in Table 4. The bond distances and angles presently obtained for ammonium hydrogen bifluoride, Table 5, are not corrected for the effects of nuclear mean-square displacements. During the least-squares refinement there were no constraints on the number of electrons in the unit cell.

Analysis of the EDD. After the refinement there were 118-(2) electrons in the unit cell, as compared to 120 for a neutral

TABLE 6: Multipole Population Parameters in NH_4HF_2

	atom						
parameter	F1	F2	N	H1	H2	H3	H4
p_v	7.43(3)	7.50(3)	5.34(5)	0.95(4)	0.84(4)	0.70(1)	0.72(1)
d_1	−2.1(3)	0	0	0	0	0.3(1)	1.2(1)
d_2	0	1.8(3)	0	0	0	0.7(1)	−1.2(1)
d_3	0	−0.6(3)	−0.3(1)	0	0	1.2(1)	−1.3(1)
q_1	0.6(1)	−0.9(1)	0.9(2)	3.8(5)	−3.4(5)	0.2(2)	0.0(2)
q_2	0	0	0.1(2)	0	0	0.6(2)	0.1(2)
q_3	0	0	0	0	0	0.6(2)	−1.2(2)
q_4	0.2(1)	−0.6(2)	0	0.3(3)	4.7(4)	0.9(2)	1.1(2)
q_5	2.0(2)	1.7(2)	−0.9(2)	−3.1(4)	2.1(5)	−0.5(2)	−0.1(2)
o_1	0.1(1)	0	0				
o_2	0	−0.3(1)	0				
o_3	0	−0.5(1)	2.1(2)				
o_4	0.3(2)	0	−3.3(2)				
o_5	−0.3(1)	0	0				
o_6	0	0.2(1)	0				
o_7	0	−0.6(1)	−0.1(1)				
h_1	0.4(1)	0.1(1)	0.1(2)				
h_2	0	0	−0.2(2)				
h_4	0.1(2)	0.1(2)	0				
h_5	0.1(1)	0.2(2)	−0.1(2)				
h_6	−	−	0.1(3)				
h_8	−0.2(2)	−0.5(2)	0				
h_9	−0.6(2)	−0.5(2)	−0.5(2)				

[a] For explanation see Table 1.

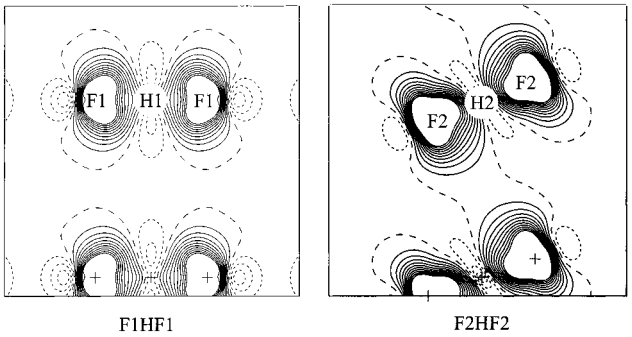

Figure 3. Static deformation density distribution in the two different F−H−F groups of NH_4HF_2. Contours are at intervals of 0.1 eÅ^{-3}. The positions of the nuclei are indicated by crosses.

TABLE 7: Assumptions and Approximations in Quantum Chemical Calculations

symbolic notation	method and approximations
RHF	restricted Hartree−Fock
LDA	density functional theory; local density approximation; Vosko et al. correlation;[25] Dirac−Slater exchange[26]
GGA	density functional theory; generalized gradient approximation; Perdew−Wang correlation;[27] Becke exchange[28]

unit cell. The population parameters in Table 6 have been scaled to give a neutral unit cell.

The monopole population parameter, p^{val}, of the fluoride atoms are 7.43(3) and 7.50(3) respectively, as compared with 8 for a true ion (see Table 6). Summation of the monopole population parameters for the hydrogen bifluoride groups gives 15.8(1) for both hydrogen bifluoride groups, as compared with 15 for a neutral hydrogen bifluoride group. Thus according to the used rigid pseudo-atom model, both hydrogen bifluoride groups are ionic with a net charge of 0.8*e*.

Figure 3 shows the static deformation EDD in the two crystallographically independent hydrogen bifluoride ions. The two distributions are very similar, although one of the ionic groups was afflicted by anharmonic thermal motion. This suggests the deconvolution procedure to be reliable. When the potential due to the EDD of the surrounding atoms was calculated for the two hydrogen bifluoride groups it immediately became clear why one group showed anharmonic thermal motion, whereas the other group did not.[19]

Calculations

Quantum Chemical Calculations. As was mentioned before, the various programs of the CRYSTAL95 package, HF and DFT, were used to perform the calculations. For the exchange correlation term in the latter, several approximation schemes are available. We compared the results obtained with HF and the local density (LDA) and generalized gradient (GGA) versions of DFT. The assumptions and approximations can be found in Table 7.

The cell dimensions and positional parameters for the atoms of NH_4F were taken from the experimental study by van Beek et al.[5] and for NH_4HF_2 from the X-ray results of Tables 1 and 4. These data are used as input in the self-consistent field calculation, together with a 6-311G** basis set.[29] The program allows the use of contraction of primitive Gaussians. The experiment showed the hydrogen atoms in the ammonium ion to be contracted, whereas the hydrogen atoms in the hydrogen bifluoride groups were not. We used this information in the CRYSTAL95 calculations, where the wave functions of the hydrogen atoms were adapted for contraction. The results of the calculations on NH_4F are shown in Figure 4.

The main differences are found between HF on one hand and DFT on the other, both in the bonding and in the core regions. The differences between the two DFT results are mainly found in the core regions (see Figure 5), where the gradient in the EDD is largest. In view of the fact that it is the introduction of the gradient in the EDD in the exchange−correlation potential that distinguishes GGA from LDA, this is not surprising.

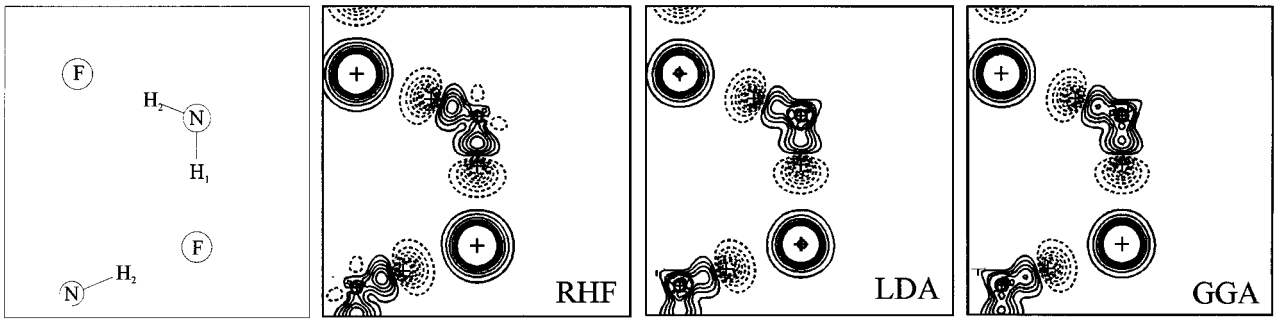

Figure 4. NH_4F. Static deformation density distribution calculated with different quantum chemical methods. Shown is the distribution in the plane of F, H1, N, and H2. The positions of the nuclei are marked by crosses. Contours are at intervals of 0.1 *e*Å^{-3}; zero contour has been omitted.

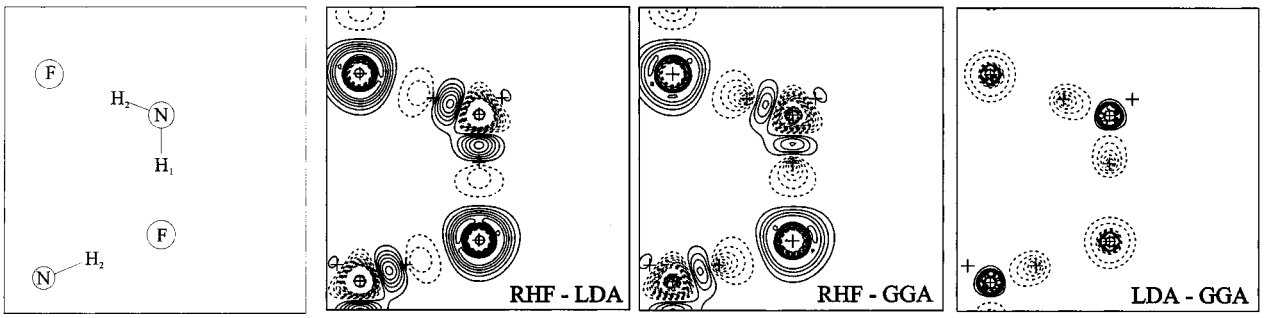

Figure 5. NH_4F. Differences between the various static quantum chemical electron density distributions. Contours are at intervals of 0.02 *e*Å^{-3}; zero contour has been omitted.

TABLE 8: Agreement Factors, *R*(*F*), between Structure Factors Corresponding to Different Ab Initio Calculations

	H (Å^{-1})						
	all	0.2	0.4	0.6	0.8	1.0	1.2
RHF vs LDA	0.64	0.70	1.02	1.26	0.94	0.29	0.33
RHF vs GGA	0.50	0.34	0.82	1.19	0.98	0.42	0.12
LDA vs GGA	0.30	0.36	0.47	0.29	0.12	0.20	0.34
number of reflections	513	4	17	37	66	101	151

[a] The agreement factors are defined in Table 3. The values given are indicated by the upper bound, e.g., $H = 0.8$ Å^{-1} indicates the range 0.6 Å$^{-1} \leq H \leq 0.8$ Å^{-1}.

The differences between the methods are also reflected in reciprocal space. Table 8 expresses these differences in *R*-factors. Again the HF method differs from the other two, and the differences in the region in reciprocal space that reflects covalent bonding are most pronounced.

Because comparison with the highly accurate experimental structure determination of NH_4F shows the GGA approximation to be the most accurate one (see section 5.1), calculations on the slightly less accurate NH_4HF_2 structure were limited to this method.

Thermal Smearing. Following the procedure outlined in section 2.3, we transformed the static structure factors calculated by CRYSTAL95 into dynamic structure factors. The thermal parameters, including anharmonic nuclear motion for atom F2 of NH_4HF_2, were taken from Table 4, whereas the corresponding data for NH_4F were taken from the experimental study of van Beek et al.[5]

The resulting dynamical theoretical structure factors were subjected to a new refinement that had to resemble the refinement of the experimental structure factors as close as possible, so *w* was set to $1/\sigma^2(F_{obs})$. In the refinement we used 8 and 67 parameters for NH_4F and NH_4HF_2 respectively: the coefficients of the multipole functions up to hexadecapoles for the N and F atoms, and multipole functions up to quadrupoles for the H atoms. The parameters for contraction, thermal motion, as well as atomic positions were kept fixed to their experimental values.

As there is no restriction on the population parameters of the atoms, the total charge of the unit cell is, in general, not zero as it should be. The refined population parameters are scaled to give a neutral unit cell. The changes in *R*-factor were negligible. At this point a multipole model fitted to the dynamical theoretical structure factors is available. The results of the refinement of NH_4HF_2 are listed in Table 9.

Theory versus Experiment

Although pseudo-atom models of both the experimental data and the dynamical theoretical data are available at this point, we still cannot compare them or their corresponding structure factors directly. The experimental model is corrected for extinction and dispersion, whereas in the theoretical case there is obviously no extinction or dispersion. The solution is to calculate the structure factors once more, this time using as input the parameters resulting from the refinement with experimental data, with the correction for extinction and dispersion set to zero. The resulting structure factors are used as the "experimental" set.

NH_4F. We first address the question of which theoretical method yields the best EDD. Because the experimental data for NH_4F are more accurate than the ones for NH_4HF_2, we focus on this compound. The difference maps that show the difference between each of the theoretical EDDs with the experimental ones, Figure 6, suggest that the DFT method is the better one. This is confirmed by a comparison in reciprocal space, where the differences are expressed in *R*-factors pertaining to shells in reciprocal space (Figure 7).

Because the GGA shows itself to be the better one in comparison with experiment, we restrict ourselves to this method in the following. A feature that deserves some attention is the deformation of the F ion. Whereas the theoretical EDDs of

TABLE 9: NH_4HF_2

	atom						
parameter	F1	F2	N	H1	H2	H3	H4
p_v	7.50(1)	7.50(1)	5.06(4)	0.86(1)	0.83(1)	0.77(1)	0.78(1)
d_1	0.8(1)	0	0	0	0	0.6(1)	1.2(1)
d_2	0	−1.1(1)	0	0	0	1.4(1)	−0.6(1)
d_3	0	−0.2(1)	0.0(1)	0	0	1.0(1)	−1.0(1)
q_1	0.3(1)	−0.1(1)	−0.0(1)	1.1(2)	−1.5(2)	−0.5(1)	0.7(1)
q_2	0	0	−0.0(1)	0	0	0.4(1)	−0.6(1)
q_3	0	0	0	0	0	0.3(1)	−1.1(1)
q_4	0.3(1)	0.5(1)	0	0.3(1)	1.1(2)	1.0(1)	0.3(1)
q_5	−0.3(1)	−0.2(1)	0.0(1)	−1.1(2)	−1.2(2)	0.1(1)	0.0(1)
o_1	−0.4(1)	0	0				
o_2	0	−0.3(15)	0				
o_3	0	−0.3(1)	1.6(1)				
o_4	0.0(1)	0	−2.0(1)		$R(F^2) = 0.8\%$		
o_5	0.3(1)	0	0		$R_w(F^2) = 1.5\%$		
o_6	0	−0.1(1)	0				
o_7	0	−0.2(1)	0.0(1)				
h_1	0.2(1)	0.2(1)	−0.0(1)				
h_2	0	0	−0.1(1)				
h_3	0	0	0				
h_4	−0.1(1)	−0.1(1)	0				
h_5	−0.1(1)	0.0(1)	0.0(1)				
h_6			0.1(1)				
h_8	−0.0(1)	−0.1(1)	0				
h_9	0.1(1)	0.0(1)	−0.4(1)				

[a] R-factors and multipole parameters resulting from a multipole refinement of the thermally smeared quantum chemical structure factors. For explanation see Table 1.

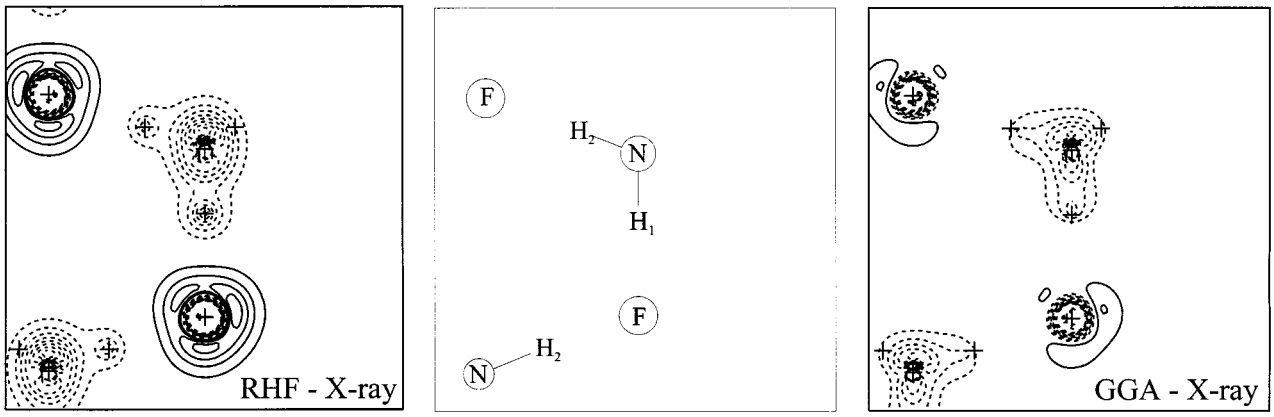

Figure 6. NH_4F. Comparison of the various quantum chemical electron density distributions (EDDs) in the plane of F, H1, N, H2, calculated according to the RHF and generalized gradient methods and the experimental EDD. Shown is the difference between thermally smeared EDD. Contours are at intervals of 0.05 eÅ^{-3}; zero contour has been omitted.

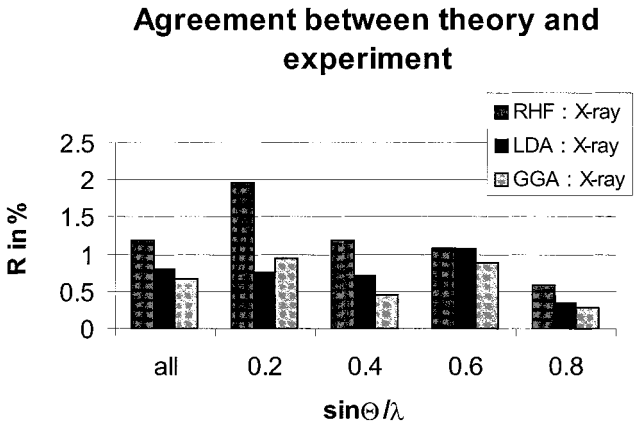

Figure 7. NH_4F. Weighted agreement factors $R_w(F)$, between the dynamic structure factors fitted to the dynamical quantum chemical intensities and those fitted to the experimental intensities. As before, the ranges are determined by the upper bound. The experimental values are compared with the values calculated with the RHF, the local density, and the generalized gradient methods.

Figure 4 suggest spherical ions, we can infer from Figure 5 that the EDD of F^- is deformed.

NH_4HF_2. To bring out various features in the EDD we show the deformation density, obtained by subtracting the sum of the neutral, isolated atoms from the total EDD. Where contracted hydrogens were used in the refinement, that is, for the H3 and H4 atoms in NH_4HF_2, contracted hydrogens were subtracted. Maps of the deformation densities in the interesting planes, that is, along (hydrogen) bonding paths, for both the experimental and theoretical models, are shown in Figure 8.

Comparing the static deformation densities, we see charge accumulations around the F and N atoms in both the theoretical and experimental cases. From the deformation maps we infer more polarization around the F atoms in the theoretical EDD than in the experimental EDD. In Figure 8a, the large dipole parameters of the F1 atoms dominate the experimental deformation density. In the theoretical EDD the dipole parameters are much smaller, which causes the contribution of the higher multipole parameters to look more pronounced in the deformation densities. Polarization effects in the two different hydrogen bifluoride groups in the experimental deformation density are very similar. In both the theoretical and experimental deformation densities, in Figure 8e and f respectively, we see an accumulation of charge at the bonding path between the N atom and the H atoms in the ammonium group. This confirms the covalent bonds that are present in this group.

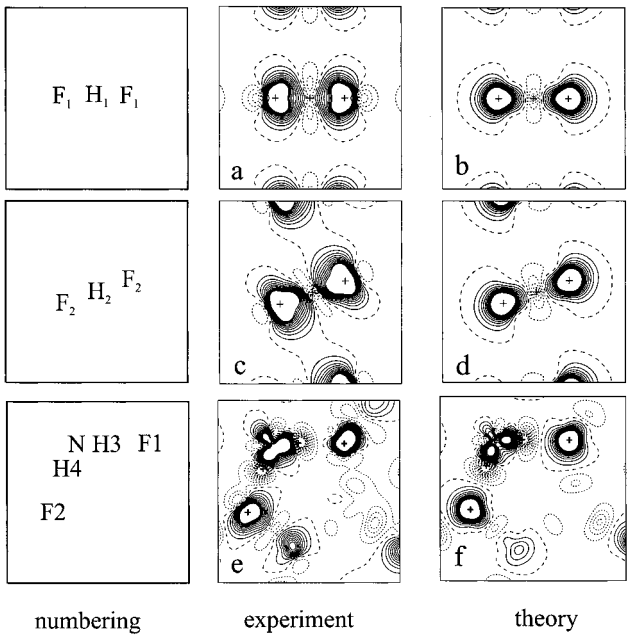

Figure 8. NH_4HF_2. Static deformation densities after refinement of experimental and theoretical data. (a) The $a-c$ plane, through the F1−H1−F1 group after refinement of the experimental data; (b) the same, but now for the theoretical data; (c) the $b-c$ plane, through the F2−H2−F2 group after refinement of the experimental data; (d) the same, but now for the theoretical data; (e) the F1−N−F2 plane after refinement of the experimental data; and (f) the same, but now for the theoretical data. Contours as in Figure 4.

The comparison can also be done in reciprocal space, that is, a comparison of the structure factors corresponding to the total EDDs from which the maps in Figure 8 are constructed. The agreement is indicated in terms of partial R-factors, and is given in Figure 9. The low-order data in this figure inform us about the agreement in the diffuse regions of the EDD.

The overall agreement factor, $R(F)$, equals 0.013, so the agreement between theory and experiment is quite good.

One of us showed in a recent paper that the comparison of theoretical and experimental data can yield problems in view of the unknown phases.[33] It is clear that in the present case these problems, for as yet unknown reasons, did not occur.

Bond Critical Points. Following Bader[4] we calculate the critical points, where the gradient of the EDD vanishes. Of special interest are the saddle points in the EDD. They appear along bonding paths and can be used to characterize the bonding. At these bond critical points we calculate the matrix of the nine

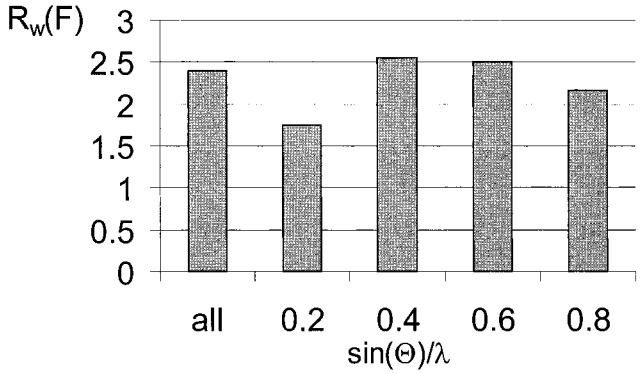

Figure 9. NH_4HF_2. Weighted agreement factors $R_w(F)$, between the dynamic structure factors fitted to the dynamical quantum chemical intensities and those fitted to the experimental intensities. As before, the ranges are determined by the upper bound.

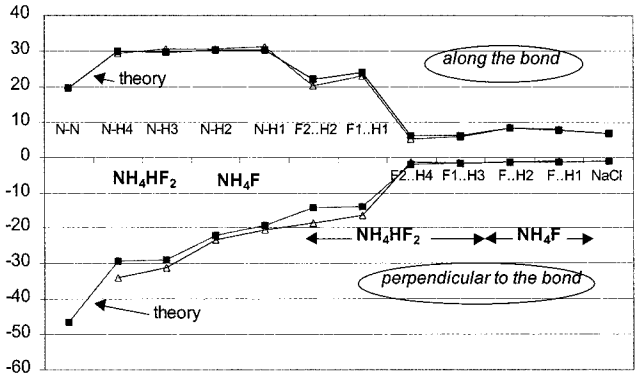

Figure 10. Curvatures of the electron density distribution at the bond critical points in NH_4F and NH_4HF_2. These curvatures are represented by the eigenvalues of the Hessian matrix. Added are the values for the typical reference compounds NaCl and N_2.

second derivatives of the EDD, the so-called Hessian matrix. Diagonalization of this matrix yields the eigenvalues λ_1, λ_2, and λ_3 expressing the curvature of the EDD in the directions perpendicular to the bond paths and along the bond, respectively. The sum of the three eigenvalues is the Laplacian. In saddle points these eigenvalues have different signs. Consequently the Laplacians have small values with relatively large errors. A negative Laplacian at the bond critical point corresponds to a concentration of electron density at that point, and thus a covalent bond. In an ionic bond the Laplacian is positive, indicating a depletion in the electron density. All results are based on the EDD calculated from the multipole density. As was stated in the *Introduction*, multipole refinement introduces a bias. This bias in the properties of the critical points was extensively discussed in a recent paper by Volkov et al.[34]

We collected the information on the critical points in both compounds in Table 10. We allege that the curvatures along and perpendicular to the bonds are more sensitive tools for characterizing bonds than the Laplacian and hence collected them in Figure 10, to which the values for N_2 and NaCl, as representatives of covalent and ionic bonding respectively,[4] are added for comparison. From Figure 10 we see that the theoretical and the experimental values correspond closely. In fact the difference between the two is for all but two points smaller than the differences between the various types of bonds.

Hydrogen Bonds. The properties of the bonds between the ammonium group and the negative ions, F^- and $(F-H-F)^-$ respectively, are similar to the properties of the Na···Cl bond, that is, both $\rho(\mathbf{r})$ and $\nabla^2\rho(\mathbf{r})$ are weakly positive. The almost vanishing curvature perpendicular to the bond supports the indication of ionic bonds: there is hardly concentration, indicating closed-shell interaction. The experimental and theoretical values of the principle values and electron densities at the critical points agree very well. Similar good agreement in hydrogen bonds was previously found by Schiott et al.[35]

The characteristics of the bonds within the hydrogen bifluoride ions differ considerably from those between the ammonium and fluorine atoms: the electron density is roughly four times larger than in Na···Cl, but also roughly four times smaller than in N≡N. The Laplacian is negative, just as in a covalent bond,

TABLE 10: Bond Critical Points (bcp's) for Ammonium Floride and Ammonium Hydrogen Bifluoride

bond	*x*	*y*	*z*	$\rho(\mathbf{r})$	$\nabla^2\rho(\mathbf{r})$	λ_1	λ_2	λ_3
experiment								
NH_4F								
N−H1	0.333	0.6667	0.2777	1.96(11)	−10(3)	−20.6(2)	−20.7(2)	31.3(17)
N−H2	0.4244	0.5740	0.4125	1.99(6)	−16(1)	−24.1(6)	−22.5(7)	30.6(8)
F···H2	0.5289	0.4696	0.4506	0.23(2)	5.6(2)	−1.3(1)	−1.3(1)	8.2(2)
F···H1	0.3333	0.6667	0.1548	0.22(5)	5.6(7)	−1.2(4)	−1.2(4)	7.9(5)
NH_4HF_2								
N−H3	0.2171	0.1789	0.3332	2.15(4)	−32(1)	−32.3(6)	−30.0(7)	30.7(6)
N−H4	0.1805	0.2827	0.5774	2.31(4)	−38(1)	−35.2(6)	−32.6(7)	29.4(6)
F1···H3	0.1696	0.0997	0.2011	0.26(1)	2.3(3)	−1.9(1)	−1.7(1)	5.9(1)
F2···H4	0.1030	0.3226	0.7224	0.21(1)	2.3(3)	−1.7(1)	−1.3(1)	5.2(1)
F1···H1	0.0326	0	0	1.29(4)	−9(1)	−16.7(6)	−16.1(6)	23.2(5)
F2···H2	0	0.47430	0.9693	1.27(4)	−17(1)	−20.1(8)	−17.0(5)	20.2(4)
theory								
NH_4F	0							
N−H1	0.3333	0.6667	0.2769	1.84	−8.7	−19.4	−19.4	30.2
N−H2	0.4247	0.5739	0.4124	1.89	−13.7	−22.7	−21.4	30.4
F··H2	0.5304	0.4687	0.4512	0.26	5.2	−1.5	−1.5	8.2
F··H1	0.3333	0.6667	0.1548	0.24	5.2	−1.3	−1.3	7.8
NH_4HF_2								
N−H3	0.2180	0.1823	0.3356	2.18	−28.2	−29.1	−28.7	29.6
N−H4	0.1843	0.2833	0.5759	2.19	−28.4	−29.3	−29.1	29.9
F1··H3	0.1813	0.1009	0.1839	0.25	2.6	−1.8	−1.7	6.1
F1··H4	0.1008	0.3183	0.7201	0.27	2.3	−1.9	−1.9	6.1
F1··H1	0.0321	0	0	1.17	−3.7	−14.2	−13.5	23.9
F2··H2	0	0.4697	0.9777	1.12	−6.3	−14.4	−13.9	22.0

[a] The electron density at the bcp's is in units eÅ^{-3} and the Laplacian at the (3,−1) bcp's is in units eÅ^{-5}. The principal values of the Hessian matrix are λ_1, λ_2, and λ_3. Estimated standard deviations are given in parentheses.

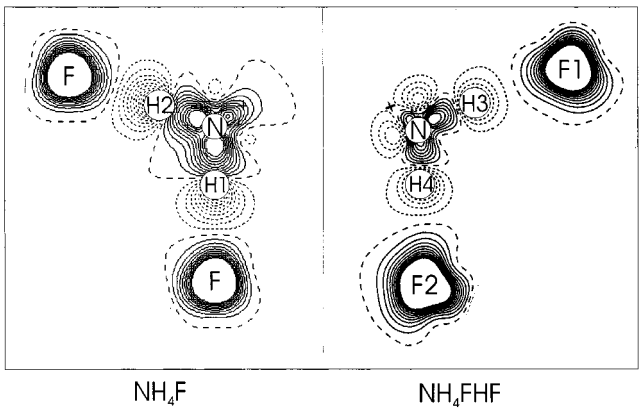

Figure 11. Static deformation density in the ammonium ion obtained from the multipoles fitted to dynamic quantum chemical structure factors for the two compounds NH_4 and NH_4HF_2. Contours are spaced by 0.05 eÅ^{-3}.

but has a rather small magnitude. More revealing are the theoretical curvatures shown in Figure 10. The two bonds show clearly intermediate character since charge is contracted to the bond path. The refinement indicated that the hydrogen atom itself is not contracted. Figure 8 shows depletion at the site of the hydrogen atom, suggesting an ionic contribution to the three-center bond. The curvatures and the charge distributions obtained from experiment support this conclusion. Flensburg et al. observed in the same way similar covalent character for the very strong hydrogen bonds in the short O−H−O hydrogen bond.

Figure 10 shows that the experimental curvature of the EDD perpendicular to the bond for the short F2···H2 bond deviates from the theoretical value. It is this group that shows the anharmonic displacement and it may well be that the deconvolution of the static EDD and the thermal motion is not complete.

The density functional calculation is seen to handle the ionic hydrogen bond and the covalent one equally well.

Ammonium Groups. Finally, we turn to the ammonium ion in ammonium hydrogen bifluoride and in ammonium fluoride and compare the deformation densities. The distances of the F atoms to the N atom are comparable for the two compounds, just as the interatomic distances in the ammonium ion. A polarization of the F atom toward the ammonium ion is apparent in both compounds. In NH_4HF_2 multipole functions up to hexadecapole functions were used to describe the fluoride ions. In NH_4F only the spherical function plus a tetrahedral function (a combination of two octopole functions) were used for the fluoride ion. As discussed before, the use of multipole functions of odd parity for this ion causes much problems in a polar space group. This difference in refinement will have some influence on the resulting deformation density in the ammonium ion and restricts somewhat the validity of the comparison of the deformation densities of the two ammonium ions, as given in Figure 11.

The charge distribution in the ammonium ion is very similar for the two compounds, that is, we see an obvious accumulation of charge between the N and H atoms, with a depletion of charge around the H atoms themselves. In NH_4HF_2 the H atoms are in the center of the depletion, whereas in NH_4F the depletion is a bit shifted toward the F atom. The spherical charge distributions, as they are given in Table 1 (NH_4F) and Table 6 (NH_4F_2H), are very much alike. Consequently we can conclude that the tetrahedral surrounding of the ammonium ion by F^- ions and the almost tetrahedral surrounding by $[F-H-F]^{-1}$ groups result in static deformation densities in the ammonium ion that are very similar.

Finally we turn to a comparison of the bond critical points, shown in Figure 10 and given in Table 10. As expected for covalent bonds, $\rho(\mathbf{r})$ is strongly positive and $\nabla^2\rho(\mathbf{r})$ is strongly negative. Because chemical experience suggests all N−H bonds to be very similar, it is rather surprising to find definite differences in the values of the curvatures in the direction perpendicular to the bonds. No differences between the groups are found in the curvature along the bonds. With the exception of the bond N−H4 the theoretical values are strongly supported by the experimental ones. Hence the transferability of the properties of critical points is less than was found by Madsen et al. for the methylammonium ion.[37]

Conclusions

In this paper we have shown that the DFT using Becke exchange and Perdew−Wang correlation functionals as implemented in the CRYSTAL95 program results in EDDs of NH_4F and NH_4HF_2 that are in very good agreement with the experimental EDD in all comparisons made: deformation density, eigenvalues of the Hessian matrix of the EDD at the critical points, and with respect to the structure factors. We have to take into account that quite some information from the experiment was used to calculate the theoretical counterpart of that experiment. We used the cell dimensions, fractional coordinates, and thermal motion of the experimental results to arrive at a set of structure factors comparable with the experimental set.

Although crystallographically different, the two hydrogen bifluoride groups are shown to be very similar in terms of the EDD, and in terms of the quantities determining the bond type in the groups. The parameters characterizing the EDD at the critical points showed the same trends in theory and experiment. The bonds in these groups show both covalent and ionic character.

The ammonium ion in NH_4F_2H shows some difference in covalent bonding with the ammonium ion in NH_4F.

References and Notes

(1) Dovesi, R.; Saunders, R. V.; Roetti, C.; Causà, M.; Harrison, N. M.; Orlando, R.; Aprà, E. CRYSTAL 95 User's Manual, 1996.
(2) Gatti, C.; Saunders, R. V.; Roetti, C. *J. Chem. Phys.* **1994**, *101*, 10686−96.
(3) Zavodnik, V.; Stash, A.; Tsirelson, V.; De Vries, R.; Feil, D. *Acta Crystallogr. B* **1999**, *55*, 45−54.
(4) Bader, R. F. W. *Atoms in Molecules, A Quantum Theory*; Clarendon Press: Oxford, 1994.
(5) van Beek, C.G.; Overeem, J.; Ruble, J. R.; Craven, B. M. *Can. J. Chem.* **1996**, *74*, 943−950.
(6) Hibbert, F.; Emsley, J. *Adv. Phys. Org. Chem.* **1990**, *26*, 255.
(7) Larson, J. W.; McMahon, T. B. *J. Am. Chem. Soc.* **1982**, *104*, 5848.
(8) Latajka, Z.; Bouteiller, Y.; Scheiner, S. *Chem. Phys. Lett.* **1995**, *234*. 159−164.
(9) Lecomte, C. Electron Density Models. In *The Application of Charge Density Research to Chemistry and Drug Design*; Jeffrey, G. A., Piniella, J. F., Eds.; Plenum Press: New York, 1991.
(10) Hehre, W. J.; Stewart, R. F.; Pople, J. A. *J. Chem. Phys.* **1969**, *51*, 2657.
(11) Hirshfeld, F. L. *Isr. J. Chem.* **1977**, *16*, 198−201.
(12) Bruning, H.; Feil, D. *Acta Crystallogr.* **1992**, *A48*, 865−872.
(13) Zachariasen, W. *Z. Phys. Chem.* **1927**, *127*, 218.
(14) Adrian, H. W. W.; Feil, D. *Acta Crystallogr.* **1969**, *A25*, 438.
(15) Terpstra, M.; Craven, B. M.; Stewart, R F. *Acta Crystallogr.* **1993**, *A49*, 685−692.
(16) El Haouzi, A.; Hansen, N. K.; LeHenaff, C.; Protas, J. *Acta Crystallogr.* **1996**, *A52*, 291−301.
(17) Pauling, L. *Z. Kristallogr.* **1939**, *85*, 380.
(18) McDonald, T. R. R. *Acta Crystallogr.* **1960**, *13*, 113.
(19) van Beek, C. G.; van Reeuwijk, S. J.; Harkema, S.; Feil, D.; Wilson, C. C.; Craven, B. M. To be published.

(20) Lehmann, M. S.; Larsen, F. K. *Acta Crystallogr.* **1974**, *A30*, 580.
(21) Blessing, R. H. *J. Appl. Crystallogr.* **1989**, *22*, 396.
(22) Rousseau, B.; Maes, S. T.; Lenstra, A. T. H. *Acta Crystallogr.* **2000**, *A56*, 300−307.
(23) Craven, B. M.; Weber, H. P.; He, X. M.; Klooster, W. T. The POP Procedure: Computer Programs to Derive Electrostatic Properties from Bragg Reflections. Technical Report TR-93-1, Department of Crystallography, University of Pittsburgh, Pittsburgh, PA, 1993.
(24) Becker, P. J.; Coppens, P. *Acta Crystallogr.* **1974**, *A30*, 129.
(25) Vosko, S. H.; Wilk, L.; Nusair, M. *Can. J. Phys.* **1980**, *58*, 1200.
(26) Dirac, P. P. M. *Proc. Cambridge Philos. Soc.* **1930**, *26*, 376.
(27) Perdew, J. P.; Wang, Y. *Phys. Rev. B* **1986**, *33*, 8800.
(28) Becke, A. D. *J. Chem. Phys.* **1988**, *88*, 1053.
(29) Krishnan, R.; Binkley, J. S.; Seeger, R.; Pople, J. A. *J. Chem. Phys.* **1980**, *72*, 650.
(30) Cromer, D. T.; Waber, J. T. In *International Tables for X-ray Crystallography*; Kynoch Press: Birmingham, 1974; Vol. 6, p 74.
(31) Clementi, E.; Roetti, C. *Atomic Data and Nuclear Data Tables*; Academic Press: New York, 1974, Vol. 14, pp 177−478.
(32) Epstein, J.; Ruble, J. R.; Craven, B. M. *Acta Crystallogr.* **1982**, *B38*, 140.
(33) de Vries, R. Y.; Feil, D.; Tsirelson, V. G. *Acta Crystallogr.* **2000**, *B56*, 118−123.
(34) Volkov, A.; Abramov, Y.; Coppens, P.; Gatti, C. *Acta Crystallogr.* **2000**, *A56*, 332−339.
(35) Schiott, B.; Iversen, B. B.; Madsen, G. K. H.; Bruice, T. C. *J. Am. Chem. Soc.* **1988**, *120*, 12117−12124.
(36) Flensburg, C.; Larsen, S.; Stewart, R. F. *J. Phys. Chem.* **1995**, *99*, 10130.
(37) Madsen, D.; Flensburg, C.; Larsen, S. *J. Phys. Chem. A* **1988**, *102*, 2177−2188.